GENERAL PHYSICS

I. MOLECULE MICROSCOPY

Academic and Research Staff

Prof. John G. King
Dr. John W. Peterson

Dr. Stanley R. Rosenthal
Dr. James C. Weaver

Graduate Students

H. Frederick Dylla
Joseph A. Jarrell

Dusan G. Lysy

Bruce R. Silver
Peter W. Stephens

RESEARCH OBJECTIVES AND SUMMARY OF RESEARCH

John G. King, James C. Weaver

Two basic types of microscopy, light and electron microscopy (and related ion versions), are well established, and are of importance to a diversity of applied and basic research problems. We are continuing our development of a new, third type, molecule microscopy, in which neutral molecules carry image-generating information from the sample. Neutral molecules are uniquely suited for probing interactions based on the chemistry of a sample; thus, molecule micrographs obtain contrast based on spatial variations of the permeability, diffusion, and binding of neutral molecules. For this reason, spatial variation in the permeation of molecules through a thin sample, diffusion along grain boundaries, binding of applied neutral molecules to a sample surface, and the existence of constituent molecules can all be revealed directly by some type of molecule microscope.

Molecule microscopy should be useful in many fields of science and engineering, particularly in materials science and biology, since molecules carrying information from the sample interact through the same weak forces that are significant in determining surface properties, and because the interactions are highly surface-specific (in contrast to photons and electrons which penetrate many atomic layers). Scientific and technological problems relating to both materials science and biology appear to be ripe for investigation by molecule microscopy. The materials science aspects of the problems have been supported by the Joint Services Electronics Program, the biological applications by the National Institutes of Health. The related molecule fluxes experiment and new molecular transducers based on immobilized enzymes have been supported by separate special grants, and in one case partially by the National Institutes of Health.

We have completed a second-generation scanning pinhole molecule microscope, a first-generation scanning desorption molecule microscope, and two related apparatus for studying relevant staining and desorption phenomena. Using these and the new molecule detectors, we are beginning investigation of problems in materials science and biology, such as grain-boundary permeabilities in various electronic and structural materials, surface staining with small molecules as a means of identifying surface sites in various materials, transport of gases and vapors in both synthetic and biological membranes, and rapid detection of small quantities of important molecules.

1. Scanning Pinhole Molecule Microscope (SPMM)

A first-generation scanning pinhole molecule microscope using H_2O molecules as the illuminant,[1] has been built and operated. This first instrument was difficult to

operate and is no longer in use. A second-generation SPMM has now been completed by Joseph A. Jarrell, and initial micrographs have been obtained using He molecules (see Sec. I-A). Since the second SPMM contains a mass spectrometer, a variety of different molecules may be used as the illuminant. At present, the resolution is ~25 μm, which should be improved to ~1 μm.

We are planning to apply this second SPMM to diffusion-permeability studies in electronic and structural materials, and also to biological samples. The new SPMM can also be used without spatial resolution by using only the rapid time response of the instrument. Preliminary results have been obtained on the O_2 consumption and CO_2 production of vascular smooth muscle in collaboration with Dr. John W. Peterson.

2. Scanning Desorption Molecule Microscope (SDMM)

The major construction on a prototype SDMM has been completed by H. Frederick Dylla and the instrument is now being tested. It includes a quadrupole mass spectrometer, an Auger electron spectrometer, and a scanning electron gun, housed in an ultrahigh vacuum system with facilities for manipulating and cleaning samples. Surface chemical information is obtained by the simultaneous use of Auger electron spectrometry (AES) and electron stimulated desorption (ESD).

The surface chemistry of a well-studied adsorbate-adsorbent system (W/O_2) is being investigated prior to the design of experiments with spatial resolution. By rastering the electron beam, images of those areas of the sample emitting specific Auger electrons, ions, or neutral molecules can be formed. The angular and velocity distributions of the species desorbed by ESD are being measured in a preliminary way, since such data may be useful in optimizing the design of the apparatus as an imaging instrument. Also, there is recent evidence[2] that ESD angular distributions may provide a new method of determining surface structures.

Other gas-surface systems to be investigated with spatial resolution include a study of the Si/O_2 system in collaboration with the molecular beam-surface studies of Dr. Mark J. Cardillo (see Sec. III) and a study of binding of H_2O to a nylon-carbon matrix as a model of hydrophilic-hydrophobic surface.

3. Desorption Experiments Related to SDMM

Recently preliminary data have been obtained by Bruce R. Silver with respect to the binding energy of alkali ions in a layer of biological material ohmically heated on a platinum alloy ribbon. Desorbed neutral molecules containing alkalis are also being studied, using surface ionization instead of an electron bombardment "universal ionizer." Of immediate interest is testing the range of validity of electron beam spot-heating calculations for thermal desorption in SDMM, as well as estimates of resolution, sensitivity, and signal-to-noise in a simply characterized system. Initial experiments are being carried out on red blood cells deposited on a metal ribbon. A long-range motivation for this approach is the problem of whether a spatial correlation of Na and K exists in transporting tissue.

In another apparatus, Dusan G. Lysy has obtained initial results on the binding of H_2O and some hydrocarbons to a dirty platinum ribbon (see Sec. I-B). This experiment is directed toward developing neutral molecule surface stains (NMSS) for SDMM. In this apparatus stain molecules can be applied and subsequently desorbed, either by ohmic heating of the platinum ribbon or locally by an electron beam. In this experiment we are investigating the binding and desorption of small molecules from platinum ribbons coated with organic molecules in order to develop NMSS for organic surfaces.

4. Molecule Fluxes through Tissue   JSEP

Under a reallocation grant of the Harvard-MIT Program in Health Sciences and Technology, Dr. Stanley R. Rosenthal has constructed a vacuum mass-spectroscopy apparatus for the study of O_2 consumption and CO_2 production in epithelial tissue. This work is in collaboration with Dr. Alvin Essig of Boston University Medical School and will be extended to nonvolatile fluxes such as lactate by the volatile enzyme product technique described in the next paragraph.

5. New Molecule Detectors

Two new rapid detectors of molecules have been developed in prototype form, and will probably have many measuring and monitoring applications. In both detectors immobilized enzymes provide the basis for a highly specific chemical reaction. In one case, detection of molecules by volatile enzyme products (VEP), very high sensitivity is obtained for a large class of enzyme reactions in which a product of the reaction is measured by techniques used in molecule microscopy. This work is described in Section I-C. In the other case, the thermal enzyme probe (TEP), the heat associated with the reaction is exploited so that the TEP can be used with any enzyme system. This work is described in Section I-D.

References

1. J. C. Weaver and J. G. King, Proc. Natl. Acad. Sci. U.S. 70, 2781 (1973).

2. J. J. Czyzewski, T. E. Madey, and J. T. Yates, Phys. Rev. Letters 32, 777 (1974).   JSEP

(I. MOLECULE MICROSCOPY)

A. SCANNING PINHOLE MOLECULE MICROSCOPE

Joseph A. Jarrell, James C. Weaver, John G. King

The construction phase of the new Scanning Pinhole Molecule Microscope (SPMM) is complete.[1] The scanning system, comprising two orthogonally mounted micrometer screws and powered TTL-programmed stepping motors, was tested optically outside the vacuum system, and has now been mounted in the main vacuum system. This system is now operating consistently in the range of 5×10^{-9} Torr and the impending addition of a titanium sublimation pump should lower this at least another order of magnitude.

During the first part of the year we worked on the VEP (volatile enzyme product) techniques, described in Section I-C, while concurrently developing peripheral apparatus for studying single cells. Neither of these applications requires spatial resolution. Most of our recent effort has been devoted to the design, construction, assembly, and testing of the scanning mechanism.
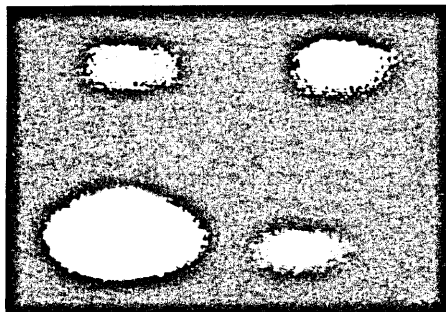

Fig. I-1.

Initial molecule micrograph of a test pattern taken with the second generation SPMM at a spatial resolution of ~25 μm. Helium gas is emitted into vacuum from 4 holes. Although the approximate diameter of the holes is 200 μm, their impedance is apparently different.

The new version of the SPMM offers better resolution (initially 25 μm; later we expect 1 μm) and mass analysis so that a molecule micrograph can be obtained with any suitable volatile molecule. For example, the recent molecule micrograph shown in Fig. I-1 was obtained with the use of helium.

References

1. J. C. Weaver and J. G. King, Proc. Natl. Acad. Sci. U. S. 70, 2781 (1973).

B. PRELIMINARY RESULTS ON THE ADSORPTION AND DESORPTION
OF WATER AND OTHER MOLECULES ON DIRTY PLATINUM AT
LOW TEMPERATURES IN A HIGH-VACUUM SYSTEM

Dusan G. Lysy

One aspect of the development of molecule microscopy[1] involves determination of the binding energy, density of binding sites, and other adsorption parameters for water and other small molecules adsorbed on various materials. These materials are spread as thin films on platinum ribbons. We report here a preliminary investigation of the adsorption characteristics of the uncoated platinum ribbons for several residual gases in the vacuum system.

The sample holder is cooled by liquid nitrogen; consequently, the nominal base temperature of the ribbon is 77°K. Adsorption from the residual gases in the vacuum system onto the platinum ribbon is allowed to occur at this ribbon temperature for a specified length of time. Resistance heating of the ribbon is then used to raise the ribbon temperature, thereby causing desorption of the adsorbed molecules. These molecules are detected by a quadrupole mass spectrometer detection system, while the ribbon temperature is monitored by a thermocouple, 2 mils in diameter, spot-welded to the center of the ribbon. Because of the exponential relationship between the rate of desorption $S(t)$ and the absolute temperature of the ribbon T, the adsorbed molecules leave the ribbon over a small range of temperatures, and as the temperature of the ribbon is raised, $S(t)$ assumes the form of a peak in the signal at that mass, appearing above a constant background signal due to the detection of the residual gases in the system.

The temperature T_p at which $S(t)$ reaches a maximum and the rate of change of temperature $\dot{T}_p$ at that point allow determination of the average binding energy E of the molecules adsorbed to the surface. At each instant the number of adsorbed molecules on the surface $n(t)$ decays with a characteristic time $\tau(T)$, which is assumed to be given by the well-known Frenkel equation:[2,3]

$$\tau = \tau_o \, e^{E/kT}, \tag{1}$$

where τ_o is often assumed[3] to be of the order of 10^{-13} s. The rate of desorption $S(t)$ is given by

$$S(t) = -\dot{n}(t) = \frac{n(t)}{\tau(T(t))}. \tag{2}$$

When $S(t)$ reaches a maximum, the condition $\dot{S}(t) = 0$ leads to the relationship
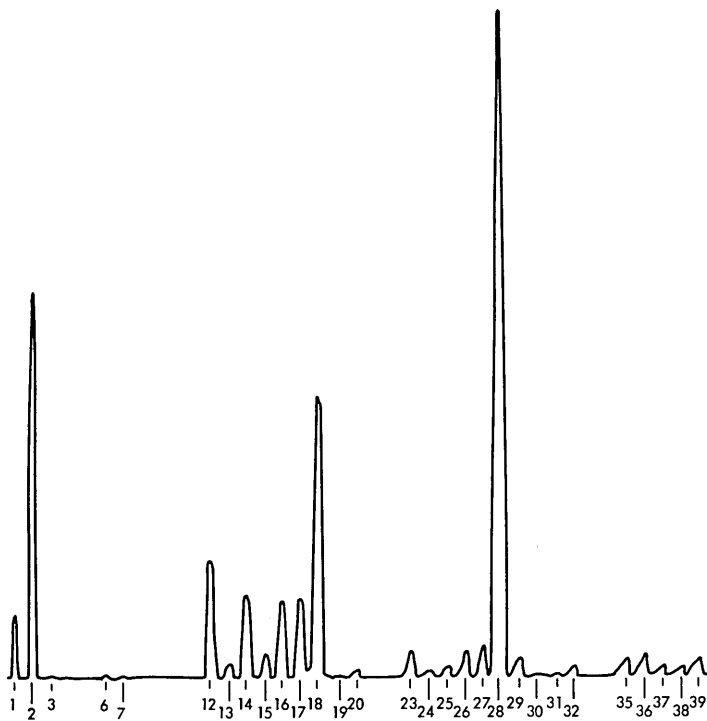
Fig. I-2.

Mass spectrum covering masses 1-39 taken at the beginning of the experiment. Total pressure = 1.0×10^{-8} Torr.
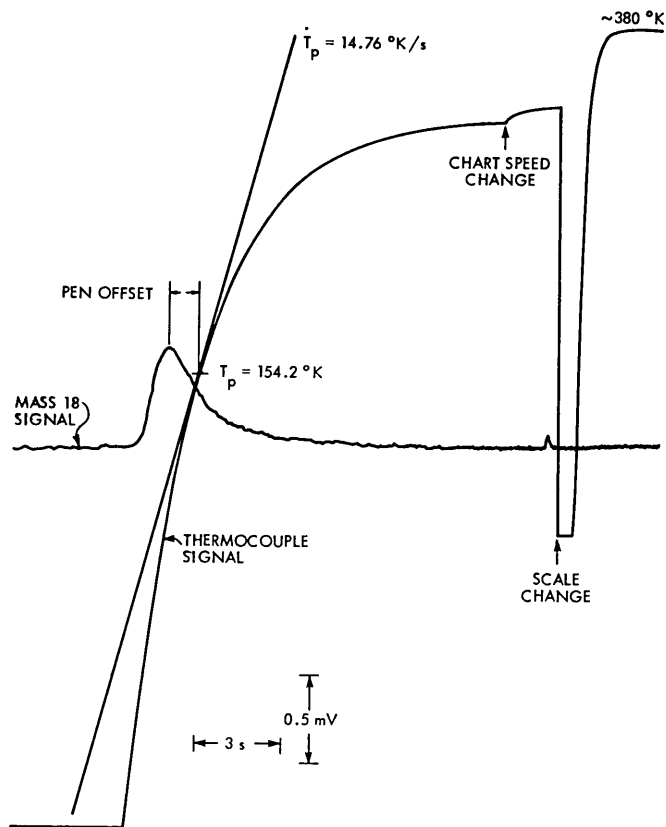

Fig. I-3. Typical water adsorption data showing mass 18 signal and ribbon temperature as functions of time during desorption.

$$\ln T_p^2/\dot{T}_p = E/kT_p + \ln \tau_o + \ln E/k. \tag{3}$$

If the heating rate is varied, T_p varies because $\dot{T}_p$ varies, and $\ln T_p^2/\dot{T}_p$ can be plotted as a function of $1/T_p$. This leads to a straight line whose slope gives the binding energy E and whose intercept allows τ_o to be estimated independently.

In our work, a platinum ribbon was cleaned following typical high-vacuum procedure: degreasing, washing with detergent, rinsing twice in distilled water, and washing in methanol, all in an ultrasonic cleaner. The ribbon was then inserted into the vacuum system. This system is a Pyrex glass cross and Viton O-ring vacuum chamber above a molecular sieve trap, pumped by a 4-inch oil diffusion pump backed by a 2-inch diffusion pump. The data were taken after the ribbon had been in the system 10 days, at
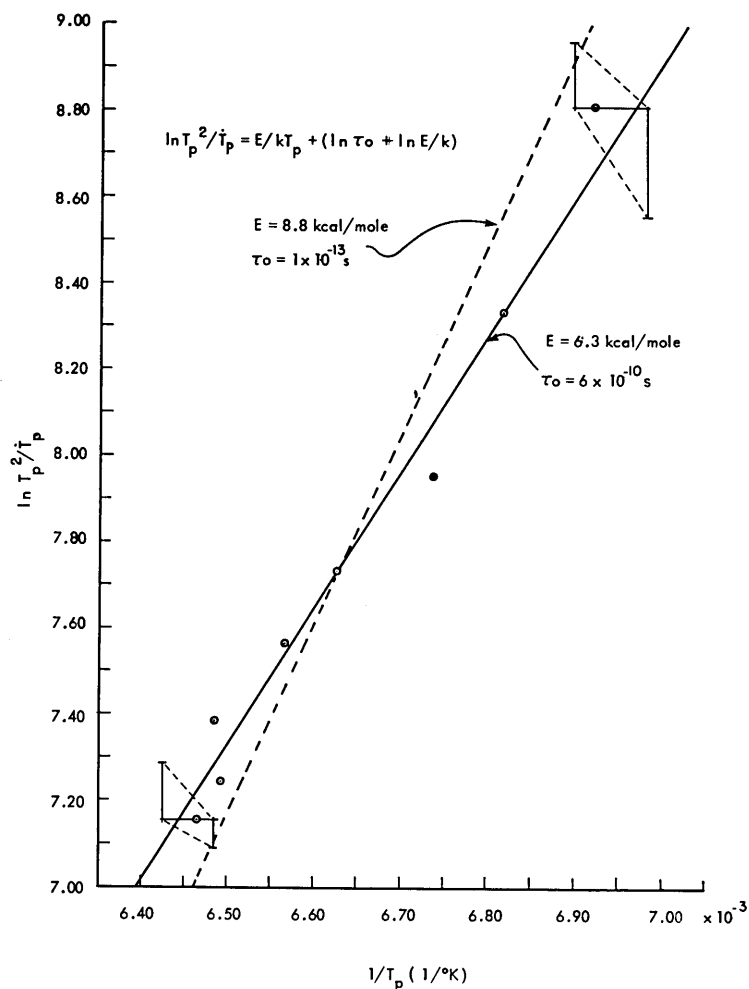

Fig. I-4. Water adsorption data plotted according to Eq. 3. Dashed line: best fit to data for assumed $\tau_o = 1 \times 10^{-13}$ s.

an average pressure of ~5×10^{-8} Torr. Thus presumably the ribbon was contaminated with the hydrocarbons that are in any unbaked vacuum system of this type. The data were taken with the liquid nitrogen traps in the system filled, at a pressure of ~1×10^{-8} Torr. The mass spectrum shown in Fig. I-2, covering only masses 1 through 39, was taken at the beginning of the experiment. The major peaks are 2 (H_2), 12 (C), 18 (H_2O), and 28 (CO).

In the water-adsorption studies the ribbon was heated to ~380°K to remove all adsorbed water (and other loosely bound molecules) and then kept at the base temperature (~77°K) for 3 minutes. Since the partial pressure of water was ~1.8 to 2.1 $\times$ 10^{-9} Torr during the experiment, the monolayer coverage time for water is estimated at 16-18 min and, therefore, the water coverage was ~0.15 to 0.20 of a monolayer at the end of the 3 minutes. The ribbon was then heated to one of a series of temperatures in the range 150-200°K, which resulted in a signal peak such as that shown in Fig. I-3. The ribbon was further heated to ~380°K to establish the standard state from which adsorption could begin again, and the whole process was repeated. In this way, a series of corresponding values of T_p and $\dot{T}_p$ was obtained. These are plotted in Fig. I-4 according to Eq. 3, and give a binding energy of $E \approx 6.3$ kcal/mole and $\tau_o \approx 6 \times 10^{-10}$ s. This binding energy is reasonable for the physical adsorption that is presumed to occur here. The best fit to the data for an assumed value of $\tau_o = 1 \times 10^{-13}$ s is also shown; as can be seen, this commonly assumed value of τ_o is at best very marginally consistent with the data. These numerical values are all preliminary, since we have not yet carried out all of the required calibrations of the measuring devices. Analysis of the peak shape is now under way to determine whether the data represent a single binding state or the average of a range of binding energies.
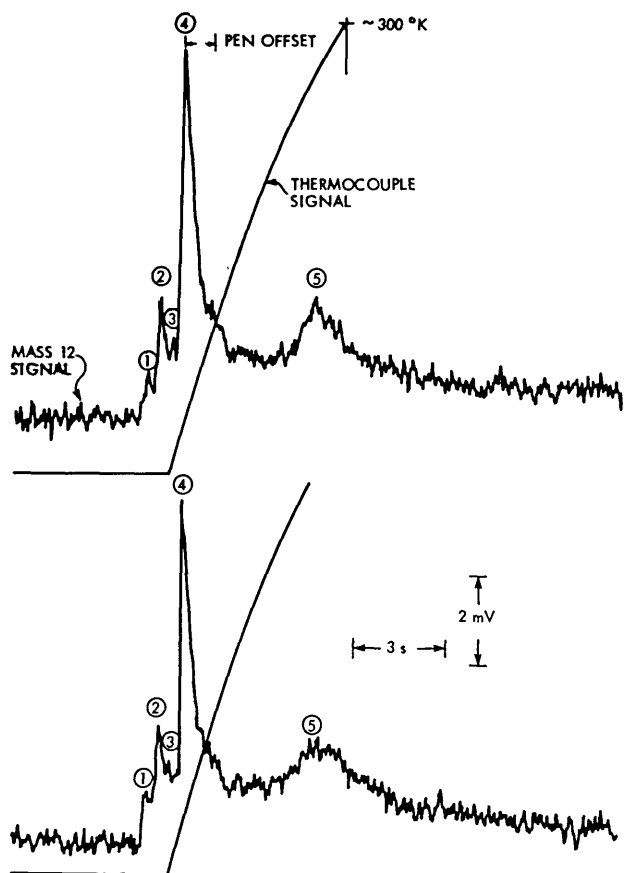

Fig. I-5.

Repeated data showing mass 12 signal and ribbon temperature as functions of time during desorption. At least 5 peaks are apparent.

Desorption signals at masses 2 (H_2), 12 (C), 16 (CH_4,NH_2), 17 (OH,NH_3), and 28 (CO) have also been observed. The carbon signal (Fig. I-5) shows extensive structure, with at least 5 separate signal peaks with values of T_p in the range 100-310°K. We believe that they represent various hydrocarbon fragments leaving the surface, and that the carbon is separated in the electron bombardment ionizer of the quadrupole mass spectrometer. This interpretation will be checked by searching for corresponding peaks at various hydrocarbon masses. In conclusion, the present data demonstrate the feasibility of this technique for the independent determination of the binding energy of τ_o for small molecules adsorbed on surfaces.

References

1. J. C. Weaver and J. G. King, Proc. Natl. Acad. Sci. U.S. 70, 2781 (1973).
2. I. Frenkel, Z. Physik 26, 117 (1924).
3. J. H. de Boer, Adv. Catal. 8, 17 (1956).

C. CHEMICAL MEASUREMENT BY VOLATILE ENZYME PRODUCTS

James C. Weaver, Martin K. Mason, Joseph A. Jarrell, John W. Peterson

We have started to develop a new instrument for the detection and measurement of molecules and present preliminary results. The basis of our approach is the combination of the sensitivity of mass spectroscopy with the specificity of enzymes that catalyze reactions with simple volatile products. In the prototype apparatus, described by J. C. Weaver in Quarterly Progress Report No. 114 (pp. 8-10), the enzyme is immobilized next to a semipermeable membrane that communicates a significant fraction of the volatile reaction product into the mass spectrometer. Since some mass spectrometers can be expected to count individual product molecules with an efficiency of ~10^{-4}, the ultimate sensitivity of this type of apparatus for substrate molecules should be ~10^{-13} molar with a time resolution of approximately 10 seconds, and the specificity of the enzyme that is employed. In one variation of this approach we expect to be able to assay the enzymes themselves with even higher sensitivity. Furthermore, this approach can be used to measure inhibitors and cofactors of enzymes.

As shown in Fig. I-6, the prototype VEP apparatus comprises a large volume (~150 ml) sample solution circulating past a layer of immobilized enzyme. The enzyme is next to a synthetic membrane, the other side of which is exposed to a vacuum system
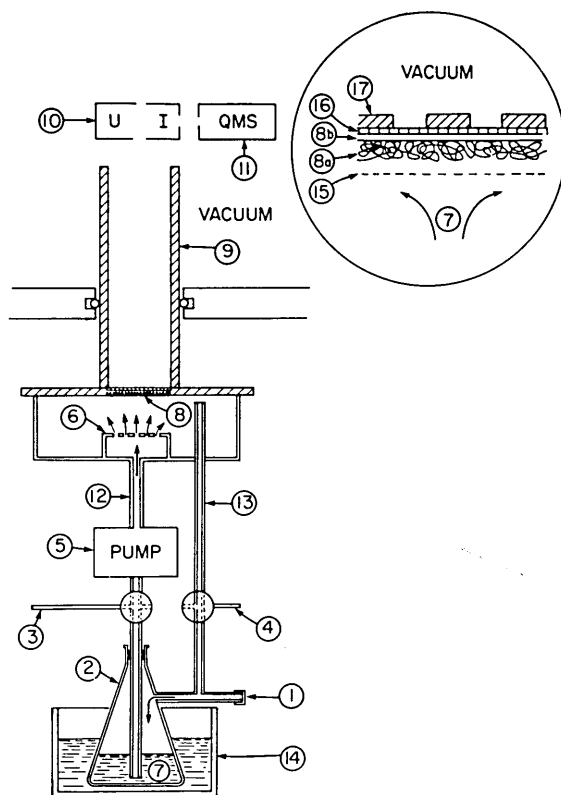
Fig. I-6. Schematic of the prototype apparatus, which comprises a circulating sample solution, an immobilized enzyme and membrane, and a mass spectrometer. (1) is a sample injection port, (2) a stirred flask for mixing, (3) and (4) inlets and outlets for partial degassing by N_2 bubbling, (5) a peristaltic pump, (6) a perforated disk providing additional mixing and more uniform delivery of the sample (7) to the enzyme layer and dimethyl silicone membrane (8). (9) is the heated transfer tube that guides the permeable and volatile molecules into (10) the ionizer of the quadrupole mass spectrometer (11). Tygon tubing was used for (12) and (13), and CO_2 absorption effects may be responsible for our inability to attain a low background. (14) is a constant (±1°C) temperature bath. The total sample solution volume was ~150 ml, and the delivery, mixing time from sample injection to the first response, was 10-20 s depending on pump speed. The inset is an enlarged schematic of the enzyme layer and membrane region for the urease experiment. Starting from the sample (7) side, a simple, one-dimensional unstirred boundary layer (15) of thickness $x \approx 10^{-2}$ cm is assumed. Then there is the ~3 × 10^{-2} cm thick polyester backing (8) of the singly backed dimethyl silicone membrane (8a) on which the enzyme is immobilized, a single piece of 1 μm pore size, 10 μm thick Nuclepore filter (16) for direct mechanical support of the membrane, followed by (17) a perforated stainless-steel disk containing six 2 × 10^{-1} cm holes for the main mechanical support, and the greatly reduced pressure ($P_{total} \approx 10^{-7}$ mm Hg) or vacuum of the mass spectrometer.

containing a mass spectrometer. The data presented in Figs. I-7 and I-8 were obtained with this simple, nonoptimal apparatus. In the first experiments we used urease which catalyzes the reaction

$$\text{urea} + H_2O \xrightarrow{\text{urease}} 2NH_3 + CO_2.$$
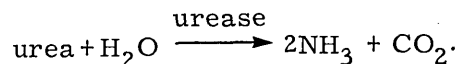
Since the molecular weight M of both NH_3 and OH (a fragment from H_2O in the mass spectrometer ionizer) is 17, we chose to measure the CO_2 count rate at M = 44. Urease was immobilized by physisorption onto the polyester fiber backing of a singly backed dimethyl silicone rubber membrane. The enzyme was then cross-linked with glutaraldehyde[2,3] after which urea was injected to increase the sample concentration stepwise. As shown in Fig. I-7 following an initial transient, the count rate exhibited a damped

Fig. I-7.
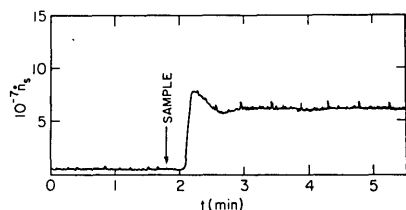
Time response of the apparatus to urea injections with urease immobilized next to the silicone rubber membrane. Following a delivery time of 16 s a transient response in the mass spectrometer count rate is observed. There is a damped oscillation, but the steady-state count rate $\dot{n}_s$ is nearly constant in time. The steady-state change $\Delta \dot{n}_s$ is used to calculate the cumulative change in $\dot{n}_s$ which in turn is plotted as a function of urea concentration in Fig. I-8.

oscillation into a final nearly steady count rate. The departure from constancy is due to the fact that as the circulation sample also accumulates the volatile product, the volatile product concentration gradient between the enzyme layer and the sample solution decreases, so that the fraction of volatiles reaching the vacuum increases. The transient is believed to be due to diffusion permeation effects associated with the unstirred layer, the enzyme layer, and the membrane, while the damped oscillation is attributed to incomplete mixing of the relatively concentrated urea injection. The steady-state count rate is nearly proportional to the steady-state enzyme catalyzed reaction rate. The change in steady-state count rate, $\Delta \dot{n}_s$, was noted as a function of urea concentration change Δs. A response curve was then determined (Fig. I-8) by plotting the cumulative $\Delta \dot{n}_s$ as a function of urea concentration. As is shown, the steady-state count rate (and enzyme catalyzed reaction rate) is proportional to urea concentration over the range 2.3×10^{-6} M to 1×10^{-3} M, and levels off above 1×10^{-3} M. The sensitivity obtained from the linear portion of the response curve is $s = \Delta \dot{n}/\Delta C = 9 \times 10^{10}$ Hz-M^{-1}.

Enzyme-catalyzed reactions producing CO_2 are particularly well suited to the VEP
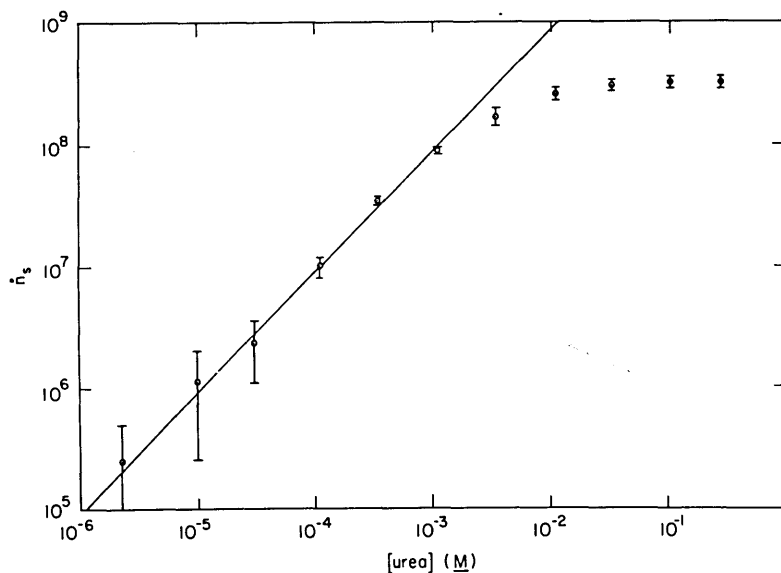
Fig. I-8. Response curve of the prototype VEP apparatus to stepwise increases in urea concentration. The ordinate represents the cumulative change in the steady-state count rate, $\dot{n}_s$, of CO_2 ions at the input of the multiplier of the mass spectrometer, while the abscissa is the cumulative urea concentration in molarity. As expected from the simple model, the response curve gives the reaction velocity directly as a function of substrate concentration for the immobilized enzyme. In the simple nonoptimal prototype apparatus a detectable response (signal to noise = 1) was first seen at [urea] = 2.3×10^{-6} M. Thereafter the response increased linearly with concentration until [urea] $\approx 10^{-3}$ M, with a leveling off into saturation, as expected for an enzyme catalyzed reaction. The straight line fit to the low concentration region was constrained to have a slope of unity, and fits the data well. The sensitivity in this region is s = 9×10^{10} counts-sec^{-1}-M^{-1}. The apparent K_M (half-maximal rate saturation constant as defined by the Michaelis-Menten kinetic model) $\approx 1.8 \times 10^{-3}$ M.

Table I-1. Single enzyme assays.

Enzyme		Reaction	Volatile
1. Pyruvate Decarboxylase	EC 4.1.1.1	pyruvate → acetaldehyde + CO_2	CO_2
2. Acetylcholinesterase	EC 3.1.1.7	Acetylcholine + H_2O → choline + acetate	Acetate
3. Uricase	EC 1.7.3.3	urate + O_2 + H_2O → allantoin + H_2O_2 + CO_2	CO_2
4. Catalase	EC 1.11.1.6	H_2O_2 + H_2O_2 → O_2 + $2H_2O$	O_2
5. Histidine Decarboxylase	EC 4.1.1.22	L-Histidine → histamine + CO_2	CO_2
6. Threonine Aldoase	EC 4.1.2.5	L-Threonine → glycine + acetaldehyde	acetaldehyde
7. Arginine Decarboxylase	EC 4.1.1.19	L-Arginine → Agmatine + CO_2	CO_2
8. DOPA Decarboxylase	EC 4.1.1.26	DOPA → dihydroxyphencylethylamine + CO_2	CO_2
9. Cysteine Desulphhydrase	EC 4.4.1.1	L-Cysteine + H_2O → pyruvate + NH_3 + H_2S	H_2S
10. Phosphopyruvate Carboxylase (ATP)	EC 4.1.1.a	ATP + oxaloacetate → ADP + phosphoenolpyruvate + CO_2	CO_2

Table I-2. Coupled enzyme assays.

Enzyme		Reaction	Volatile
1. Lactate Dehydrogenase	EC 1.1.1.27	L-Lactate + NAD → pyruvate + NADH	pyruvate $\xrightarrow{4.1.1.1}$ CO_2
2. Barbiturase	EC 3.5.2.1	Barbiturate + $2H_2O$ → malonate + urea	urea $\xrightarrow{3.5.1.5}$ CO_2
3. Tryptophase	EC 4.2.1.e	L-Tryptophan + H_2O → pyruvate + NH_3 + indole	pyruvate $\xrightarrow{4.1.1.1}$ CO_2
4. L-Serine Dehydratase	EC 4.2.1.13	L-Serine + H_2O → pyruvate + NH_3 + H_2O	pyruvate $\xrightarrow{4.1.1.1}$ CO_2
5. Glucose Dehydrogenase	EC 1.1.1.47	β-D-Glucose + NAD → D-glucono-δ-lactone + NADH	NADH $\xrightarrow{1.1.1.1}$ ethanol
6. Glucose-6-Phosphate Dehydrogenase	EC 1.1.1.49	D-G-6-P + NADP → D-glucono-δ-lactone 6 phosphate + NADPH	NADH $\xrightarrow{1.1.1.1}$ ethanol
7. Sarcosine Oxidase	EC 1.5.3.1	Sarcosine + H_2O + O_2 → glycine + HCHO + H_2O_2	HCHO $\xrightarrow{1.2.1.1}$ formate
8. Xanthine Oxidase	EC 1.2.3.2	Xanthine + H_2O + O_2 → urate + H_2O_2	urate $\xrightarrow{1.7.3.3}$ CO_2
9. Glucose Oxidase	EC 1.1.3.4	β-D-Glucose + O_2 → D-glucono-δ-lactone + H_2O_2	H_2O_2 $\xrightarrow{1.11.1.6}$ O_2
10. Octopine Dehydrogenase	EC 1.5.1.a	Octopine + NAD + H_2O → arginine + pyruvate + NADH	pyruvate $\xrightarrow{4.1.1.1}$ CO_2

method, since the diffusion constant of CO_2 in H_2O is reasonably large and the permeability of dimethyl silicone membranes to CO_2 is large ($P_M = 1.3 \times 10^{-2}$ cm-sec^{-1} for a membrane that is 1.3×10^{-3} cm thick). Some other fairly simple molecules also appear to be sufficiently diffusable, permeable, and volatile, so that a diversity of enzymes may be suitable (Table I-1). Furthermore, there is the obvious possibility of applying coupled reactions (Table I-2) in which the product of the first reaction is the substrate for the second. For example, lactate may be measured with CO_2 as the volatile by lactate dehydrogenase and pyruvate decarboxylase.

The VEP technique appears to be suitable for measurement of certain enzymes, coenzymes or enzyme inhibitors. For example, if we use a two-compartment system with immobilization by entrapment, then substrate can be provided at high concentrations in one and the sample fluid passed through the other. For simplicity, assume that S permeates readily through the membrane separating the two compartments to provide $S \gg K_M$ so that any enzyme molecule that is present will produce volatile product molecules at the turnover number $1 \lesssim \nu_T \lesssim 10^4$ s^{-1}. For a given configuration, the count rate will be ν_T larger when enzyme molecules rather than substrate molecules are treated as the unknown, and the expected sensitivity will improve proportionately. Also, it may prove attractive to use mass labeled compounds (not necessarily radioactive) in which the enzymatically liberated volatile product contains the label, for example, C^{14}. Because of the long half-life ($\sim 5 \times 10^3$ yr) of C^{14} only $\sim 4 \times 10^{-7}$ of the C^{14} nuclei in a sample decays in one day, whereas with the VEP method we should be able to achieve counting efficiencies of 10^{-4} in much shorter times (less than 1 minute).

In conclusion it appears that there are many potential applications for the VEP technique ranging from clinical and environmental measurements to research and monitoring applications involving very small quantities or very low concentrations of the sample.

We have enjoyed valuable discussions with Drs. C. L. Cooney, A. Essig and S. R. Caplan.

References

1. M. K. Mason, S. B. Thesis, Department of Physics, M. I. T., 1974 (unpublished).

2. R. Haynes and K. A. Walsh, Biochem. Biophys. Res. Commun. 36, 235 (1969).

3. C. L. Cooney, J. C. Weaver, S. R. Tannenbaum, D. V. Faller, A. Shields, and M. Jahnke, in E. K. Pye and L. G. Wingard, Jr. (Eds.), Enzyme Engineering, Vol. 2 (Plenum Press, New York, 1974), p. 411.

4. T. E. Barman, Enzyme Handbook (Springer Verlag, New York, 1969).

D. THERMAL ENZYME PROBE: A NEW ENZYMATIC TRANSDUCER

Boehringer Mannheim GmbH

Scott P. Fulton, James C. Weaver, Charles L. Cooney, Steven R. Tannenbaum, Peter Schuler

[Dr. Cooney and Dr. Tannenbaum are members of the Nutrition and Food Science Department, M. I. T. Dr. Schuler is affiliated with Boehringer Mannheim GmbH.]

The application of enzymes to chemical analysis has had considerable impact already on the development of very specific measurement systems. A major limitation to the widespread use of enzymes for chemical analysis has been the need to interface an enzyme-catalyzed reaction with an appropriate sensor. We report recent progress in the development of a technique for chemical analysis that incorporates the advantages of using enzymes and has the potential for application to any enzyme-catalyzed reaction. Specifically, we employ calorimetry and exploit the enthalpy change that is common to all chemical reactions. Thus enzymes provide specificity and calorimetry provides universality. The application of calorimetry to chemical analysis is a well-established technique.[1] Unfortunately, most of the systems are difficult to use in routine chemical analysis. We have used an approach based on a thermal enzyme probe (TEP), which is applicable to either discrete or continuous sampling and has a relatively rapid time response. Preliminary work on this technique has been described elsewhere.[2]

The Thermal Enzyme Probe is a pair of thermal sensors, onto one of which an active enzyme is immobilized. The thermal sensors are thermistors that form half of a high-precision Wheatstone bridge that is sensitive to the temperature difference, ΔT, between the thermsitors.[3] When the thermistor pair that constitutes the probe is placed in a solution containing the substrate for the enzyme, the enzyme-catalyzed reaction only occurs in a region near the thermistor with the enzyme, and a ΔT develops between the thermistors. The magnitude of the steady-state ΔT, and therefore of the bridge output, is proportional to the steady-state reaction rate at the enzyme-coated thermistor. Thus the steady-state ΔT measured by this technique is applicable to the analysis of any chemical for which there is an enzyme that can be immobilized next to one of the thermal sensors.

A simple model serves to estimate the expected steady-state ΔT as a function of substrate concentration. Furthermore, it allows identification of the critical parameters for interpretation of experimental results. Some assumptions are made for simplicity. We begin by noting that the substrate flux density, J_s, from the bulk solution to an assumed monolayer of enzyme is given by

$$J_s = \frac{D}{x}(S_o - S),\qquad\qquad(1)$$

where D is the substrate diffusivity, S_o and S are its concentration in the bulk solution
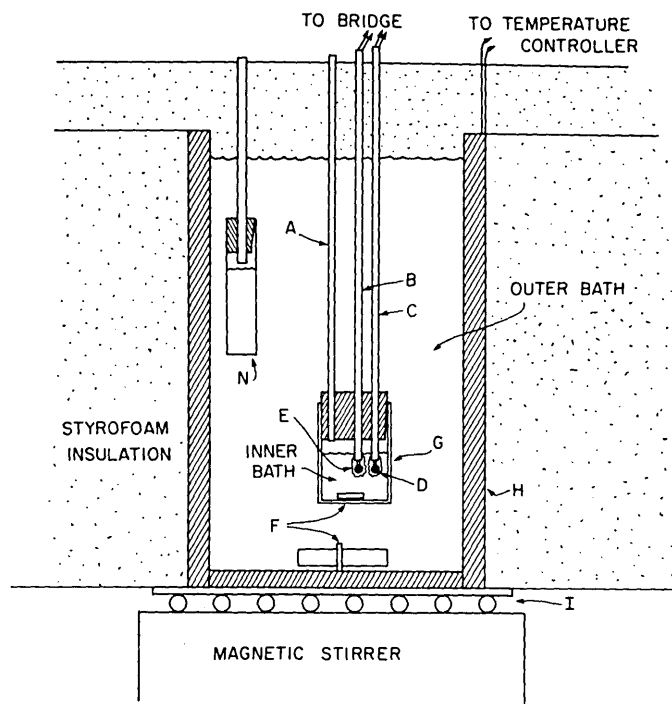
Fig. I-9. Apparatus used for the thermal enzyme probe data shown in Fig. I-10. A is the sample delivery tube, B and C are the two stainless-steel tubes containing thermistors D and E, F refers to the two magnetic stirring bars, G is the glass wall of the inner bath, H is the metal, temperature-regulated wall of the outer bath, and N is a small glass container holding the concentrated sample or blank (buffer).

and at the enzyme, and x is the boundary-layer thickness. The boundary layer is treated as a stationary, unstirred, aqueous layer plus any trapped water or porous gel surrounding the active enzyme. The heat flux density J_Q, which is conducted away from the probe, is

$$J_Q = K\Delta T/x, \tag{2}$$

where K is the thermal conductivity of water, and ΔT is the temperature difference between the probe and the bulk solution. The rate of reaction, V, at the probe surface is assumed to be given by the Michaelis-Menten model:

$$V = (V_m S)/(K_m + S), \tag{3}$$

where V_m is the maximum reaction rate per area, and K_m is the concentration of substrate at one-half of V_m. Note that both V and V_m are expressed here as the rate per unit surface area. For $S \ll K_m$, Eq. 3 may be simplified to

$$V \approx (V_m/K_m)S. \tag{4}$$

Since $J_s = V$, and the enthalpy of reaction is ΔH, at steady state $V\Delta H = J_Q$, and we find

$$\Delta T \approx \left\{ \frac{\left(\frac{D}{x}\right)\left(\frac{V_m}{K_m}\right)}{\left(\frac{D}{x}\right) + \left(\frac{V_m}{K_m}\right)} \left[\frac{x\Delta H}{K}\right] \right\} S_o. \tag{5}$$

Writing ΔT in this form shows explicitly that in the linear region where $S \ll K_m$, we can model the enzyme layer as a sink for substrate which is connected in series with an effective conductance (V_m/K_m) and a real conductance (D/x). Frequently $V_m/K_m \gg D/x$ so that in this case

$$\Delta T \approx \left(\frac{D\Delta H}{K}\right) S_o, \tag{6}$$

and ΔT is proportional to the bulk concentration of the substrate. It is important to note that the ΔH in Eq. 6 results from all of the reactions that occur in the region of the TEP. This includes the reaction(s) catalyzed by the enzyme(s) and, for example, heat of protonization associated with the buffer.[3] If the assumptions of our simple model are realized, it follows that in the linear region the reaction is diffusion-limited, and neither the enzyme concentration at the surface nor the boundary layer thickness is important in determining ΔT.

This model also predicts time response because of substrate diffusion of order $\tau \approx x^2/2D \approx 10$ s for a well-stirred system in which $x \approx 10^{-2}$ cm. Since thermistors immersed in water typically have thermal time constants of 1-2 s, it can be seen that τ fundamentally limits the response. In the present apparatus (Fig. I-9) the time constant for heat exchange between the inner and outer bath is approximately 40 seconds. This additional effect dominated the TEP transient response because of the common mode response (with respect to ambient temperature) of the thermistor pair when we added a sample or blank at a slightly different temperature. Thermal sensors with a significantly better common mode rejection can be used to minimize this effect so that the time response will then be limited by τ.

By substituting typical values in Eq. 6, we can estimate the expected ΔT for a given substrate concentration S_o. Typically, if heats of protonization are included, for S in the 10^{-3} $\underline{M}$ range the model predicts values of ΔT in the range 10^{-5} to a few times 10^{-4} °C for the case of a stationary boundary layer. Effects associated with a boundary layer executing laminar flow, however, can increase the ΔT. Some of the
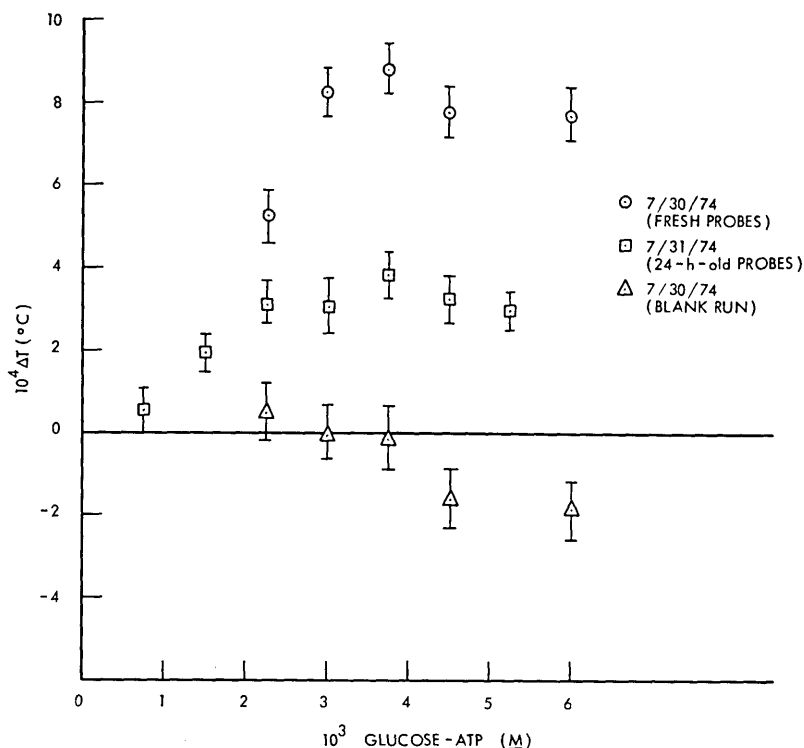
Fig. I-10. Response of the thermal enzyme probe to injections of equal concentrations of glucose and ATP. ⊙ is the response of TEP with fresh hexokinase, △ a blank response taken the same day, and ⊡ the response after 24 hours. The decline in activity is similar to that observed by others for the gluta-raldehyde immobilization used here.

results obtained with the apparatus shown in Fig. I-9 are presented in Fig. I-10.

The major problems in TEP involve the physics of suitable differential thermometry. In particular, experiments have shown that the current limitation is hydrothermal noise sensed by the large thermistors (bead diameter ≈ 2 mm) in a "well stirred" flow with turbulence added, as well as a rather poor common mode rejection ratio (CMRR ≈ 10) of the thermistors with respect to ambient temperature. Electrical noise is not limiting. We are exploring the use of high-temperature coefficient miniature resistors fabricated on a common silicon chip. Such thermal sensors offer the combined advantages of small size and excellent CMMR with respect to temperature. By using this approach, it appears feasible to obtain a minimum detectable ΔT of order 10^{-6} °C, which for typical enzyme systems implies a minimum detectable substrate concentration of order 10^{-5} M.

The high-precision circuitry for this experiment was designed by James Williams, Department of Nutrition and Food Science, M. I. T.

References

1. H. D. Brown, Biochemical Microcalorimetry (Academic Press Inc., New York, 1969).

2. C. L. Cooney, J. C. Weaver, S. R. Tannenbaum, D. V. Faller, A. Shields, and M. Jahnke, in E. K. Pye and L. Wingard (Eds.), Enzyme Engineering, Vol. 2 (Plenum Press, New York, 1974).

3. A. Johansson, J. Lundberg, B. Mattiasson, and K. Mosbach, Biochim. Biophys. Acta 304, 217 (1973).